A Human-inspired Simulator for the Study of Orientation and Balance Control

ÁNGEL CANELO, INÉS TEJADO,
JOSÉ EMILIO TRAVER, CRISTINA NUEVO,
BLAS M. VINAGRE
Industrial Engineering School
University of Extremadura
Avenida de Elvas, s/n 06006 Badajoz
SPAIN
{itejbal,jetraverb,bvinagre}@unex.es

JAVIER PRIETO-ARRANZ
School of Industrial Engineering
University of Castilla-La Mancha
Avenida Camilo José Cela, s/n 13071 Ciudad Real
SPAIN
Javier.PrietoArranz@uclm.es

Abstract: Biologically, the vestibular feedback is indispensable to the ability of balancing for both humans and humanoid robots in different conditions. This paper presents a human-inspired orientation and balance control of a three degree-of-freedom (DOF) simulator that emulates a person sitting in a platform. In accordance with the role in humans, the control is essentially based on the vestibular system (VS), which regulates and stabilizes gaze during head motion, through modeling the behavior of the semicircular canals and otoliths in the presence of stimuli, i.e., linear and angular accelerations/velocities derived by the turns experienced by the robot head on the three Cartesian axes. The semicircular canal is used as the angular velocity sensor to perform the postural control of the robot. Simulation results in the MATLAB/Simulink environment are given to show that the orientation of the head in space (roll, pitch and yaw) can be successfully controlled by a proportional-integral-derivative (PID) with noise filter for each DOF.

Key–Words: Vestibular system, Model, Robot, Simulation, MATLAB.

1 Introduction

Human balancing ability requires both visual and vestibular feedback. To this respect, there has been a considerable progress over the last years to identify, understand, and model the underlying mechanisms of human postural control, especially for applications in robotics [9, 16].

In humans, the vestibular system (VS), along with other sensory and motor systems, is responsible for three cognitive functions that support mobility: it helps humans to maintain the balance of the body, to stabilize the head, and, when the body or head is in motion, to maintain the visual gaze on a target. Hence, the VS runs as a sensor of the angular motions (more precisely, by means of the semicircular canals) and translational motions (thanks to the otoliths), so that the human body can use all the information collected by such a system to maintain balance, perceive the environment and control its position. These functions show the great importance of the VS for human life. Bearing these human skills in mind, the robotics community is currently progressing towards developing objective standards, among which defining benchmarks that allow objective comparisons [9]. Likewise, advances in such skills may also help to the progress of, for example, robotic rehabilitation devices. The work presented in this paper is a first step towards the former of the mentioned applications.

The design of a biologically-inspired artificial VS as a sensor for controlling robot heads during motion has received a great interest in robotics to regulate and stabilize gaze. Complete models of eye-head stabilization based in human skills have been addressed in e.g. [5, 7, 8, 12, 19, 20, 21]; most of them include the model validation on humanoid robots. These are just a few examples of the investigations that can be found in the literature. Furthermore, it has been demonstrated that the balance of robots that are not endowed with a vestibular sensor is clearly inferior that of humans [10].

The objective of this work is to design and develop a balance control based on the human VS of a three degree-of-freedom (DOF) robot that emulates a person sitting in a platform or chair. More precisely, position of the head (or gaze) of the robot has to be controlled during its motion. For that purpose, a model of the robot will be developed in the MAT-

LAB/Simulink environment. The robot head will include a model of the VS, which will be essentially constituted by the semicircular canals and otolithic organs. The orientation of the head in space (roll, pitch and yaw) will be controlled by a proportional-integral-derivative (PID) controller, using the semicircular canal as angular velocity sensor.

There is thus a double motivation for this research. The principal motivation is to emulate human balancing ability on a 3-DOF robot from a model of the human VS. The second motivation is to show that classical PID controllers can perform successfully the orientation of the robot head using vestibular feedback from the semicircular canals.

For simulations, the stimulation of the VS will be carried out to observe the behaviour of the semicircular canals and otoliths as follows: semicircular canals will be stimulated by the angular velocities obtained from the kinematic model of the robot, whereas otoliths (otolithic macula) will be stimulated by linear accelerations.

The remainder of the paper is organized as follows. Section 2 summarizes the human VS from both physiological and mathematical points of view. Section 3 is devoted to the simulator of the 3-DOF robot that has been developed to study orientation and balance control. Section 4 contains the simulation results obtained when controlling the robot with classical PID controllers. Conclusions and future applications are drawn in Section 5.

2 Human Vestibular System

This section describes the human VS from both physiological and mathematical points of view.

2.1 Physiological background

The VS is a cuboid cavity located in the inner ear, specifically in the center of the bony labyrinth. It is formed by the vestibule and the semicircular canals. Inside the vestibule there are two membranous structures [3]: the utricle and the saccule. In these structures, there are peripheral receptor organs, called macules (Figure 1(a)), which are composed of sensory ciliated receptor cells covered by a horizontal membrane on which there is a series of calcium carbonate crystals. These crystals, called otoliths, are very susceptible to linear accelerations or decelerations in the three planes of space because of the density difference between the otoliths and the macula. The magnitude and direction of the resulting shearing force acting on

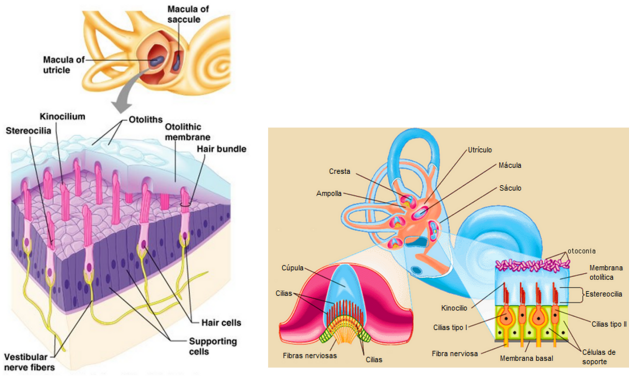

Figure 1: Illustrations of human ear physiology: (a) macule of the utricle and the saccule (image extracted from [2]) (b) outside and inside of the semicircular canals (image extracted from [4]).

the receptor cells depends upon the magnitude and direction of the linear acceleration stimulus relative to the macula. In each inner ear the two otolithic receptor regions in the utricle and the saccule are approximately orthogonal to one another, allowing almost any direction of linear acceleration stimulus to be transduced.

In what concerns the semicircular canals, there are tree, one horizontal and two vertical [3]. They are cylindrical tubes that form two thirds of a circumference and are oriented in the three planes of space, so that the plane of each of them forms with the other two a 90° angle (Figure 1(b)). The semicircular canals are filled with a pristine fluid called endolymph. The stimulation factor of the semicircular canals are angular accelerations, either by rotation of the head or rotation of the whole body.

Likewise, the semicircular canals lead into the vestibule at their two extremes, one of which, called ampulla, has a double diameter, whereas the other is where the recipients of rotations, the ampular crests, reside. These crests are covered by a gelatinous substance rich in mucopolysaccharides, called cupula.

2.2 Mathematical modeling

Next, we are going to focus on the mathematical models of semicircular canals and otoliths, which are the essential components of the VS.

2.2.1 Semicircular canals

Angular motion sensation relies on inertial forces, caused by head accelerations, to generate endolymph

Table 1: Parameters of the semicircular canal model [13].

Parameter	Value	Description
k	6.8 Gpa/m^3	stiffness of the cupula coefficient
m	1070 g/cm^4	mass of the fluid contained in the canal
d	0.76 g/cm	inertial force coefficient
τ_1	13.2 s	time constant
τ_2	6 ms	time constant

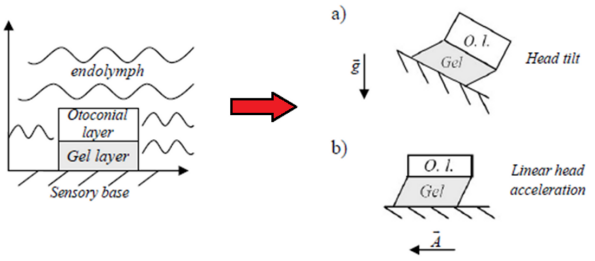

Figure 2: Schematic diagram of the performance of the otolith organ: (a) Stimulus inclination of the head (b) Inertial stimulus. Image extracted from [15].

fluid flow within the toroidal semicircular canals. This fluid flow is described by the torsion pendulum model. Hence, it describes the semicircular canals as a second-order overdamped system governed by the following differential equation [13]:

$$m\frac{\mathrm{d}^2Q}{\mathrm{d}t^2} + c\frac{\mathrm{d}Q}{\mathrm{d}t} + kQ = f, \qquad (1)$$

where Q is the displaced volume in endolymph, m is the mass of the fluid contained in the canal, c denotes the damped viscous effect in the conduit, k is the stiffness of the cupula, and f is an inertial force.

After taking the Laplace transform of (1) and doing the corresponding unit changes, the following transfer function can be obtained for semicircular canals to relate the volume displaced by the cupula (in cm^3) with the angular velocity of the head (rad/s):

$$T_{ssc}(s) = \frac{Q(s)}{\omega(s)} = \frac{ds/m}{\left(s+\frac{1}{\tau_1}\right)\left(s+\frac{1}{\tau_2}\right)}, \qquad (2)$$

where d is the inertial force coefficient, and τ_1 and τ_2 are the time constants of the system. The values of m, d and the time constants are shown in Table 1; they were taken from [13].

2.2.2 Otoliths

Many models have been developed for the understanding of normal otolithic function taking into account its mechanical properties, most of them derived from experimental studies on the physiological effects of a tilt stimulus on the otoliths by recording responses of single primary afferent neurons from the utricle and the saccule. Reviews on the topic can be found in [1, 6].

Among them, the most repeated model considers the otolith as a second-order mass damping system, where the otoconia layer is modeled as a rigid solid. Moreover, the gel layer is modeled as a viscoelastic isotropic material and the endolymph, as a Newtonian fluid with uniform viscosity (see Figure 2). Refer to [14, 15] for more details.

After doing some simplifications in the otolith mechanical dynamics, Ormsby [11] proposed a model for the response of the otolith afferent dynamics as

$$G(s) = \frac{AFR(s)}{F(s)} = \frac{33.3\,(10s+1)}{(5s+1)\,(0.016s+1)}, \qquad (3)$$

which relates the transmission of nerve signals from the otolith (afferent firing rate, AFR) with a gravito-inertial force f, or the linear acceleration (m/s^2).

Concerning model (3), it should be remarked that:

1. the values of its parameters were taken from [17];
2. in this work, its input will be the acceleration obtained from the kinematic model together with the linear acceleration that is considered to have the head of the robot due to linear motion (if this is considered).

3 The Robot Simulator

This section describes the simulator of a 3-DOF robot developed for the study of orientation and balance control.

Figure 3(a) illustrates the robot that will be considered in this work. As can be seen, it consists of a person sitting on a chair or platform that rotates with a certain angular velocity. This person experiences a stimulation of the sense of balance, rotation that will be assimilated by the semicircular canals (specifically by the lateral canal) in such a way that a displacement of the endolymph fluid will occur. Kinematic model of the robot and its implementation in MATLAB/Simulink are explained next.

3.1 Kinematic model

The kinematic model is due to the fact that, while the chair rotates, it is admitted that the person can turn the head on the three axes X, Y, and Z (roll, pitch and

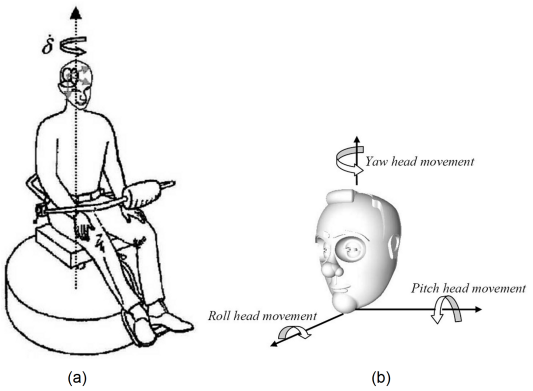

Figure 3: Illustration of the simulator: (a) a person is sitting on a platform that rotates with a certain angular velocity with the sense of balance assimilated by the semicircular canals (b) details of turns of the head on the three axes: roll, pitch and yaw.

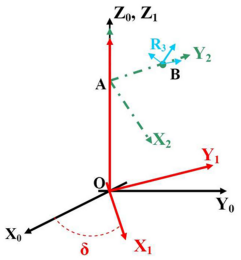

Figure 4: Reference systems: system R0 (O, X_0, Y_0, Z_0) (terrestrial system), system R1 (O, X_1, Y_1, Z_1) (system associated with the chair), system R2 (A, X_2, Y_2, $Z2_2$) (system associated with the head), system R3 (B, X_3, Y_3, Z_3) (system associated with semicircular canals if they are not considered orthogonal).

yaw), as shown in Figure 3(b). The rotation angles on the three axes are denoted as α, β, and γ, respectively. This effect will be added to the one produced by the rotation of the chair, whose angle of rotation is δ.

To work with this kinematic model, let consider the reference systems shown in Figure 4. The aim is to obtain the components of the angular acceleration vector (which is transformed to an angular velocity prior to being introduced in the semicircular canal model) and the components of the linear acceleration vector. Both components need to be expressed in the reference system R0 (terrestrial or reference system) as of the angular velocity vector of the chair in R1 and the angular velocity vector of the head in R2 (both known).

The angular velocity vector corresponding to the chair rotation in R1 is $\bar{\omega}_1 = (0, 0, \dot{\delta})$. Then, the angular velocity of the chair can be calculated in R0 by means of

$$\bar{\omega}_{1/0} = M_\delta \bar{\omega}_1, \tag{4}$$

where M_δ is the transformation matrix of the two reference systems, which is defined as:

$$M_\delta = \begin{pmatrix} \cos\delta & \sin\delta & 0 \\ -\sin\delta & \cos\delta & 0 \\ 0 & 0 & 1 \end{pmatrix}. \tag{5}$$

The motions of the head are defined by the angular velocity vector in R2, i.e., $\omega_2 = (\dot{\alpha}, \dot{\beta}, \dot{\gamma})$. Then, the angular velocity of the head can be expressed in R0 as

$$\bar{\omega}_{2/1} = M_\alpha M_\beta M_\gamma M_\delta \bar{\omega}_2, \tag{6}$$

where the transformation matrices of the reference systems are given as follows:

$$M_\alpha = \begin{pmatrix} 1 & 0 & 0 \\ 0 & \cos\alpha & \sin\alpha \\ 0 & -\sin\alpha & \cos\alpha \end{pmatrix}, \tag{7}$$

$$M_\beta = \begin{pmatrix} \cos\beta & 0 & -\sin\beta \\ 0 & 1 & 0 \\ \sin\beta & 0 & \cos\beta \end{pmatrix}, \tag{8}$$

$$M_\gamma = \begin{pmatrix} \cos\gamma & \sin\gamma & 0 \\ -\sin\gamma & \cos\gamma & 0 \\ 0 & 0 & 1 \end{pmatrix}. \tag{9}$$

Thus, the total angular velocity vector can be obtained in R0 by

$$\bar{\omega}_{2/0} = \bar{\omega}_{2/1} + \bar{\omega}_{1/0}, \tag{10}$$

i.e., adding the contributions of the angular velocity of the head and the angular velocity of the chair, both expressed in R0.

Likewise, to obtain the angular accelerations in the system R0, we proceed in the same way as before: adding the two contributions, the total angular acceleration vector in R0 is given by

$$\bar{\dot{\omega}}_{2/0} = \bar{\dot{\omega}}_{2/1} + \bar{\dot{\omega}}_{1/0}. \tag{11}$$

However, since the kinematic model admits the possibility of considering non-orthogonal semicircular canals (reference system R3), a last transformation can be done to express the angular accelerations with this non-orthogonal orientation. This transformation can be expressed by

$$\bar{\dot{\omega}}_{B2/1} = M_\phi M_\theta M_\psi \bar{\dot{\omega}}_{2/0}, \tag{12}$$

Table 2: Euler angles that define the perpendicular of each canal.

Canal	ψ **(rad)**	β **(rad)**	ϕ **(rad)**
Anterior	2.212	0.177	0
Lateral	2.336	0	−0.274
Posterior	0	−0.331	0.038

where M_ϕ, M_θ, and M_ψ are the transformation matrices for the system R3. The angles ϕ, θ and ψ represent the Euler angles that define the normal to the plane of each canal (lateral, posterior and anterior). The values of these angles are shown in Table 2.

The rotations also give rise to components of linear acceleration (A) that contribute to stimulate the otoliths. The terms that make up the linear acceleration vector at point B (origin of the R3 system, where the VS is located) can be expressed as

$$\bar{A}_{B2/0} = \bar{A}_{B2/1} + \bar{\dot{\omega}}_{1/0} \times \bar{AB} \qquad (13)$$
$$+\bar{\omega}_{1/0} \times \left(\bar{\omega}_{1/0} \times \bar{AB}\right) + \bar{A}_{coriolis},$$

where $\bar{AB} = \begin{pmatrix} 0 \\ 0.03 \\ 0 \end{pmatrix}$ (in m), $\bar{A}_{B2/1} = \bar{\dot{\omega}}_{2/1} \times \bar{AB}$, and $\bar{A}_{coriolis}$ is the acceleration due to the Coriolis acceleration term.

3.2 Implementation in MATLAB/Simulink

Figure 5 shows the appearance of the 3-DOF robot in Simulink. Its implementation can be divided into two parts: the kinematic model of the robot including the VS, and the postural control. Details of each part are given next.

3.2.1 Kinematic model with vestibular system

The block diagram of the kinematic model of the robot with the VS is shown in Figure 6. As can be observed, it is composed by the following main subsystems:

- The subsystem *Kinematics* simulates the kinematic model explained in the previous section. The components of the angular acceleration vector resulting from this subsystem, either expressed in the system R0 (consideration of orthogonal semicircular canals) or in the system R3 (consideration of non-orthogonal semicircular canals), are integrated to obtain the angular velocity vector and, subsequently, each component of this vector is introduced into the transfer function (2). As a result, the volume of the endolymph displaced by the cupula in the three semicircular canals (posterior, anterior and lateral) is obtained.

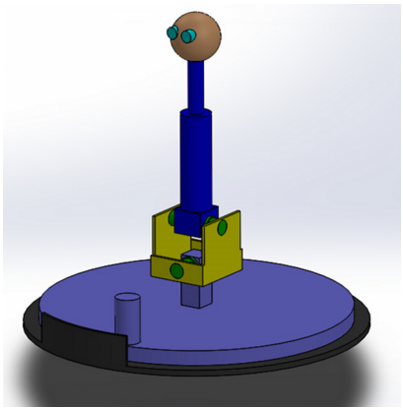

Figure 5: Appearance of the 3-DOF robot in Simulink.

- The linear acceleration vector that will be introduced in the otolith transfer function (3) is obtained by the subsystem *Utricle & saccule*.

The connection between the two main blocks is due to stimulation of the VS: the outputs of both the kinematic model of the robot and the utricle and saccule, namely, angular and linear accelerations, respectively, are the inputs to the dynamic model of the VS. This model, in turn, is composed by the model of semicircular canals, which will be stimulated by the angular velocities, and the one corresponding to otoliths (otolithic macula), which will be stimulated by the linear accelerations.

It should be remarked that it is possible to choose if the person also experiences a translation motion. In this case, another vector of linear acceleration will be added to the linear acceleration vector obtained from the angular motion (the one that has been calculated in the subsystem *Kinematics*).

3.2.2 Postural control

The robot is on a rotating platform and in turn can make three turns emulating the turns of the head (roll, pitch and yaw). For this purpose, the robot has two joints and, in turn, the head allows the relative rotation with the part where it is held. The 3D model of the robot illustrated in Figure 5 was obtained using blocks of the toolbox Simscape Multibody^{TM}

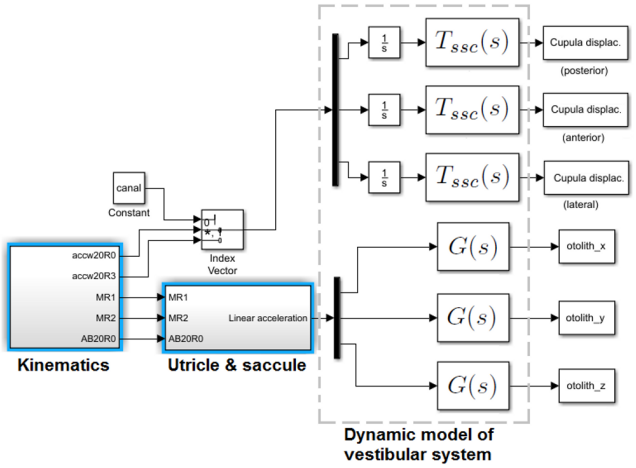

Figure 6: Kinematic model with VS in Simulink.

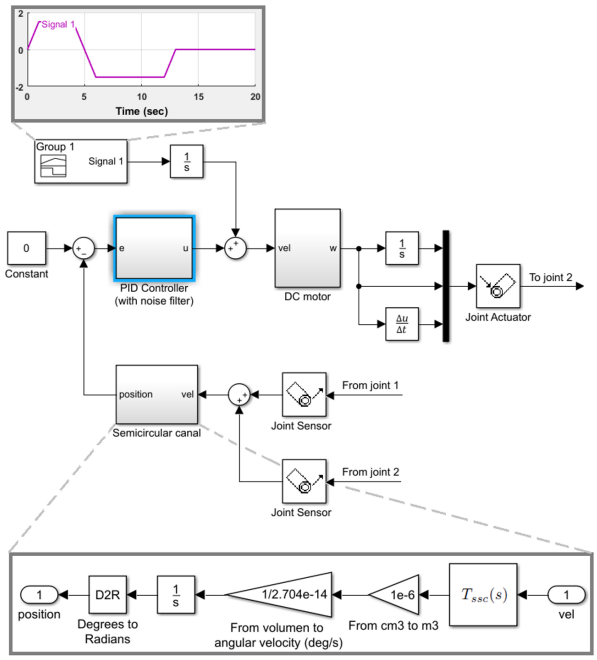

Figure 7: Closed-loop diagram to control the angular position of each joint of the robot in Simulink.

(formerly SimMechanics^{TM}) of MATLAB. Simscape Multibody^{TM} provides a multibody simulation environment for 3D mechanical systems [18]. In this work, each part/piece of the robot was firstly built in 3D by Solidworks.

The control system of the robot consists of a closed-loop with a PID controller with noise filter for each DOF (control position), as shown in Figure 7. As can be seen, the reference is 0 rad in the 3-DOF. Likewise, the rotations of the other joints are added as disturbances in the system in every control loop. It should be noticed that:

1. The subsystem *Semicircular canal* is used as a sensor to measure the angular position of the corresponding DOF.

2. The head motion is emulated by means of a disturbance that is added to each loop.

3. Although the DC motor model requires an angular velocity as input, it also responds to an angular position. This is because the angular velocity which is going into the subsystem *Semicircular canal* is obtained from a joint sensor, which provides the angular velocity of the joint (in rad/s).

4. The control loop is the same for each degree of freedom in the rotation over $X-$, $Y-$ and $Z-$axis, except that in the rotations over X and Y only the disturbance of the control signal must be compensated (motion of the robot in those axes). Hence, there is no other contribution to the rotations over $X-$ and $Y-$axis; the rotation of the platform only affects to the rotation over $Z-$axis.

4 Simulations

This section is devoted to the simulations of the 3-DOF robot developed in Simulink. For illustration purposes, results of the kinematic model with the VS are firstly given. Then, the corresponding to the whole robot are discussed.

Figure 8 shows the graphical user interface (GUI) that was created in MATLAB in order to interact with the simulator of the robot. As can be observed, the window contains: on the left, the components and plots related with the VS; on the right, the controllers for each DOF can be tuned. In what the VS is concerned, the following options are configurable before simulating (from top to bottom and left to right): 1) orthogonal or non-orthogonal semicircular canals; 2) the head motion can be considered, or not; 3) the shape of the angular velocity of the rotating chair can be selected as constant, trapezoidal or sinusoidal; 4) the kind of the angular velocity of the head for each axis can be selected as roll, pitch, yaw or combined; 5) it is possible to consider, or not, linear acceleration; and 6) otolith responses can be plotted or not. With respect to the robot, a 3D animation is shown. Likewise, it is also possible to see postural errors.

Simulations results are given below, firstly considering only the kinematic model of the robot with the VS and then for postural control. It is important to remark that the values of the proportional, integral and

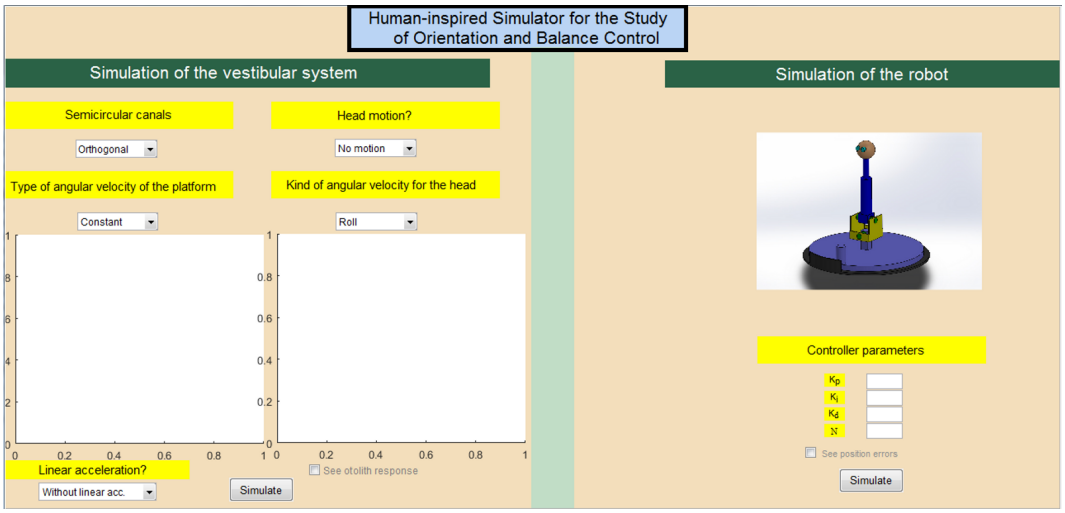

Figure 8: Graphical user interface developed for the simulator.

derivative gains of the PID controllers used in simulations were tuned empirically.

4.1 Kinematic model with vestibular system

In this section, several simulations of the Simulink model shown in Figure 6 will be carried out for different angular velocities as stimulus for both the chair/platform and the head rotation.

Figure 9 illustrates the volume displaced in the semicircular canals when the chair moves with a constant angular velocity of 1.7 rad/s, starting at 1 second. For the orthogonal consideration (Figure 9(a)), it is clear that only the lateral canal is stimulated since the rotation of the chair stimulates the rotation on $Z-$axis of the head (yaw). For the non-orthogonal case (Figure 9(b)), the lateral canal suffers the greatest stimulation. However, both the anterior and posterior canal also suffer a volume displacement, although less than the lateral and in a different direction.

Regarding otoliths, the behaviour is shown in Figure 10 with and without considering translational motion. For the latter (Figure 10(a)), it can be seen that the greatest stimulation in terms of AFR is on $Z-$axis due to the acceleration of gravity, being on $X-$ and $Y-$axis negligible by comparing the order of magnitude. Likewise, when considering translational motion with a linear acceleration vector whose components in the three axes have a trapezoidal function starting at 3 seconds and ending at 7 seconds with a maximum value of 1 m/s^2, it can be observed from Figure 10(b) that now the stimulation on $X-$ and $Y-$axis is much greater due to the acceleration. The greatest stimulation is still on $Z-$axis because of gravity.

Furthermore, if we now consider that the head experiences different rotations in the different axes at the instants $t = 10$ s and $t = 25$ s, the displaced volumes in the semicircular canals are shown in Figure 11 for the orthogonal and non-orthogonal cases. For the former (Figure 11(a)), it can be stated that each semicircular canal is stimulated with the component of the angular acceleration vector that corresponds to its respective orthogonal axis (anterior with the component Y; posterior with the component X; lateral with component Z). In addition, the lateral canal first suffers volume displacement due to the angular acceleration produced by the chair in the head, and then that of the turn over the $Z-$axis (yaw) of the robot head at instants $t = 10$ s and $t = 25$ s. In the case of non-orthogonal canals, as can be observed from Figure 11(b), a volume displacement is produced in the three canals with the rotating motion of the chair, which is obviously greater in the lateral canal. However, at the rotation instants, the anterior and posterior canals begin to experience a larger volume displacement that is obviously caused by the component of the angular acceleration vector of the head that coincides with the orthogonal axis of the respective semicircular canal. The lateral canal suffers a displacement of volume very similar to the case of orthogonal canals.

4.2 Postural control

A simulation of the whole model of the robot will be carried out; the error signals will be obtained in terms of angular position (in degrees).

The reference for the angular velocity of the plat-

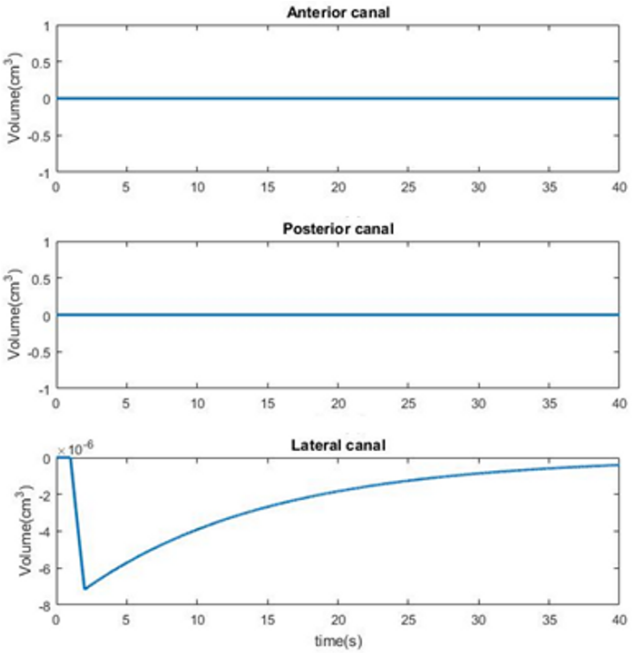

(a)

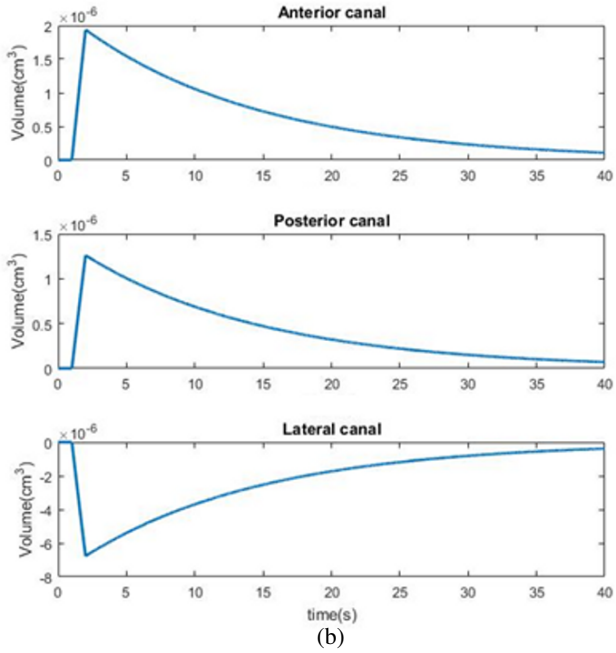

(b)

Figure 9: Volume displaced in the semicircular canals: (a) orthogonal case (b) non-orthogonal case.

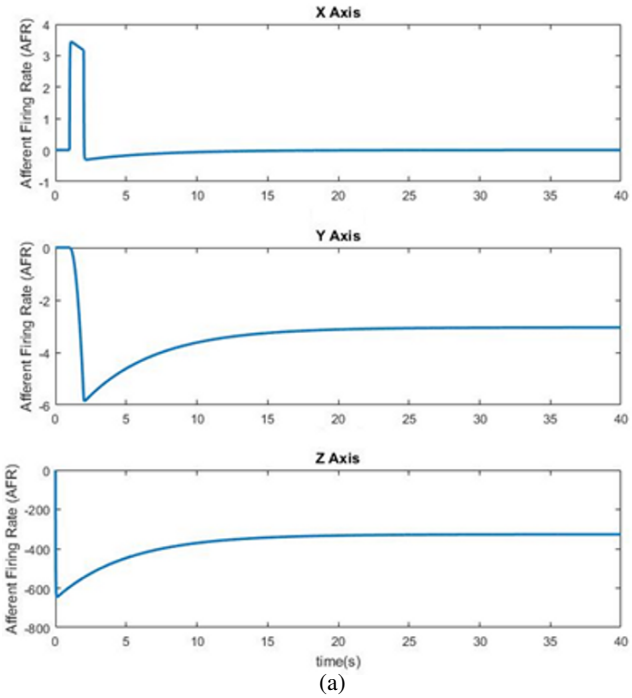

(a)

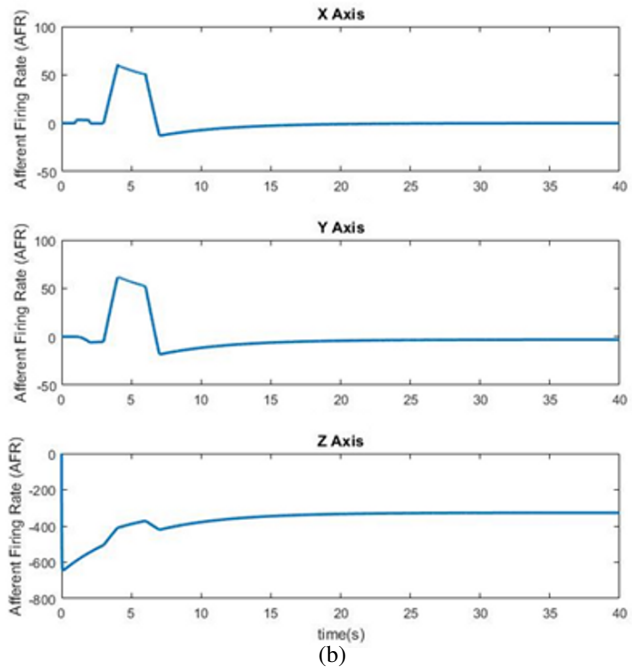

(b)

Figure 10: AFR on $X-$, $Y-$, and $Z-$axis of otoliths: (a) with no translational motion (b) with translational motion.

form can be seen in Figure 12(a), whereas the reference for the angular velocities of the robot over the three axes are equal and has the form shown in Figure 12(b). Simulation results are obtained for two different control cases, in which only the integral part of the PIDs will be changed. Let subscripts X, Y, and Z denote the controller applied to the DOF corresponding to $X-$, $Y-$, and $Z-$ axis, respectively. The cases considered are: case 1) the controller parameters are $K_{i_{X,Y}} = K_{i_Z} = 5$; and case 2) the controller parameters are $K_{i_{X,Y}} = K_{i_Z} = 8$. In both scenarios, $K_{p_{X,Y,Z}} = 2$, $K_{d_{X,Y,Z}} = 1$, and $N_{X,Y,Z} = 50$.

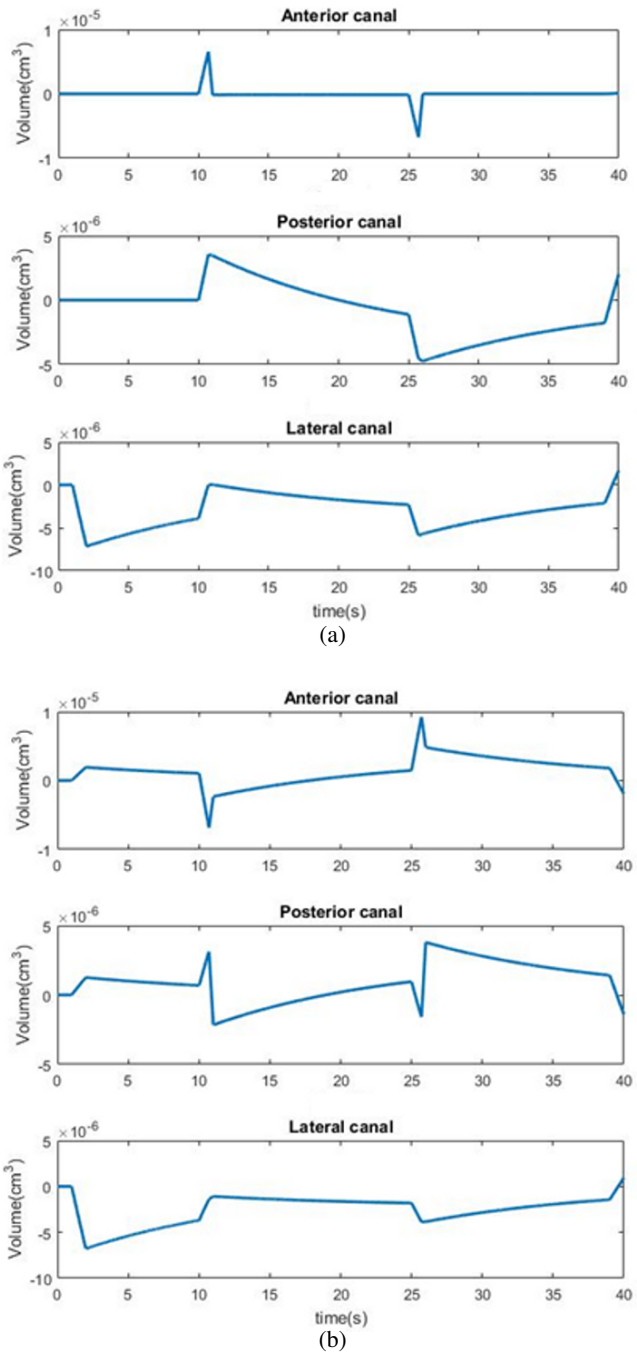

Figure 11: Volume displaced in the semicircular canals considering rotations in the head: (a) orthogonal case (b) non-orthogonal case.

Figure 13 shows the error when controlling the robot with the mentioned PIDs. In Figure 13(a), it can be observed how the controller tries to take the error to 0 degrees and, when the turns end, a constant error different from 0 is achieved (there is a small steady state error due to the disturbances added). The error

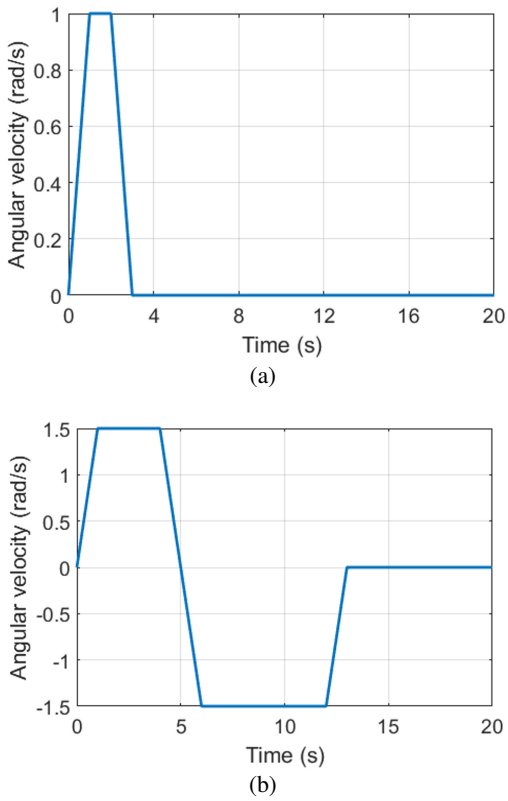

Figure 12: Reference angular velocity for: (a) platform (b) X, Y, Z axes of the simulator. (Notice that the scale of y-axis is not the same).

on $Z-$axis is obtained by adding the angle rotated by the platform plus the angle rotated by the robot head (which have opposite sign), since this DOF must compensate the rotation of the platform. The result of this sum should be zero or very close to zero. But for the second scenario, a lower stationary error is obtained, as well as lower overshoot (see Figure 13(b)).

5 Conclusion

This paper has presented the balance and orientation control of a three degree-of-freedom (DOF) simulator that emulates a person sitting in a platform based on the human vestibular system (VS) to regulate and stabilize gaze during head motion. The VS was essentially modeled through the behavior of the semicircular canals and otoliths in the presence of stimuli, i.e., linear and angular accelerations/velocities derived by the turns experienced by the robot head on the three Cartesian axes. The semicircular canal was used as the angular velocity sensor to perform the postural control of the robot.

In accordance with the role in humans, simulation

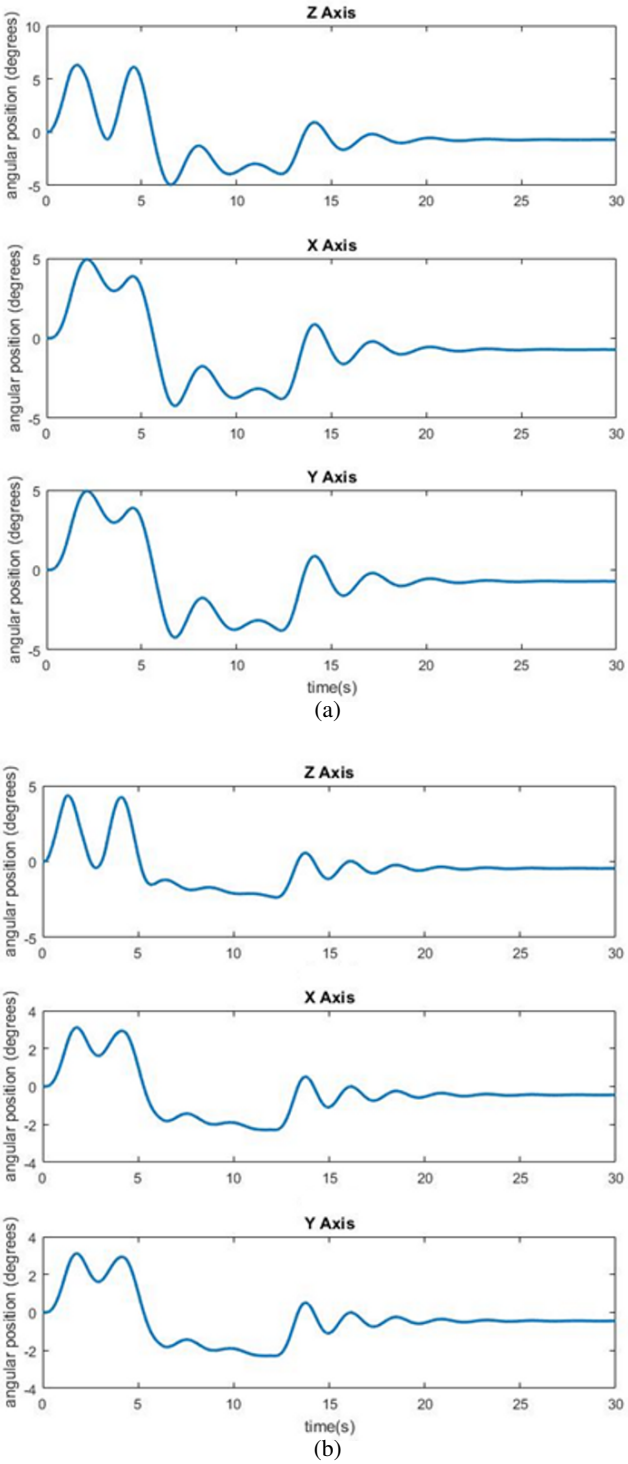

Figure 13: Error signal on each axis for different PID controllers: (a) Case 1 (b) Case 2.

results in the MATLAB/Simulink environment were given to show the importance of the VS to control the orientation of the head in space (roll, pitch and yaw). The simulator was controlled by a proportional-integral-derivative (PID) with noise filter for each DOF.

Future applications explore the possibility of using artificial VSs on human heads, as an indirect interface between humans and robots, for telecontrol. The semicircular canals may be built by a 3D printer and fill them with a liquid with properties similar to the endolymph. Thus, the displaced volume of liquid and hence the angular velocity could be measured.

References:

[1] Houshyar Asadi, Shady Mohamed, Chee Peng Lim, and Saeid Nahavandi. A review on otolith models in human perception. *Behavioural Brain Research*, 309:67–76, 2016.

[2] Benjaming Cummings. Interactive physiology, 2005. [Online] http://nedbook.adam.com/pages/ipweb/home/.

[3] Terry D.Fife. *Handbook of Clinical Neurophysiology*, volume 9, chapter Overview of anatomy and physiology of the vestibular system, pages 5–17. Elsevier, 2010.

[4] Inc. Encyclopæ dia Britannica. Online encyclopædia britannica. [online] https://www.britannica.com/.

[5] Egidio Falotico, Nino Cauli, Przemyslaw Kryczka, Kenji Hashimoto, Alain Berthoz, Atsuo Takanishi, Paolo Dario, and Cecilia Laschi. Head stabilization in a humanoid robot: models and implementations. *Autonomous Robots*, 41(2):349–365, 2017.

[6] R. Jaeger and T. Haslwanter. Otolith responses to dynamical stimuli: results of a numerical investigation. *Biological Cybernetics*, 90:165–175, 2004.

[7] Ravi Kaushik, Marek Marcinkiewicz, Jizhong Xiao, Simon Parsons, and Theodore Raphan. Implementation of bio-inspired vestibulo-ocular reflex in a quadrupedal robot. In *Proceedings 2007 IEEE International Conference on Robotics and Automation*, pages 4861–4866, 2007.

[8] Ory Medina, Daniel Madrigal, Félix Ramos, Gustavo Torres, and Marco Ramos. A new approach for body balance of a humanoid robot. *International Journal of Software Science and Computational Intelligence*, 6(4):1–14, 2014.

[9] Thomas Mergner and Vittorio Lippi. Posture control–Human-inspired approaches for humanoid robot benchmarking: Conceptualizing tests, protocols and analyses. *Frontiers in Neurorobotics*, 12(21):1–16, 2018.

[10] Thomas Mergner, Georg Schweigart, and Luminous Fennell. Vestibular humanoid postural control. *Journal of Physiology-Paris*, 103(3):178–194, 2009.

[11] Charles C. Ormsby. *Model of Human Dynamic Orientation*. PhD thesis, Massachusetts Institute of Technology, 1974.

[12] F. Patane, F. C. Laschi, H. Miwa, E. Guglielmelli, P. Dario, and A. Takanishi. Design and development of a biologically-inspired artificial vestibular system for robot heads. In *Proceedings of 2004 IEEE/RSJ International Conference on lntelligent Robots and Systerns*, pages 1317–1322, 2004.

[13] R. D. Rabbitt, E. R. Damiano, and J. W. Grant. *The Vestibular System*, chapter Biomechanics of the Semicircular Canals and Otolith Organs, pages 153–201. Springer, 2004.

[14] P. Selva, J. Morlier, and Y. Gourinat. Development of a dynamic virtual reality model of the inner ear sensory system as a learning and demonstrating tool. *Modelling and Simulation in Engineering*, 2009:Article ID 245606, 10 pages, 2009.

[15] Pierre Selva. *Modeling of the vestibular system and nonlinear models for human spatial orientation perception*. PhD thesis, Institute of Aeronautics and Space, University of Toulouse, 2009.

[16] Karim A. Tahboub. Biologically-inspired humanoid postural control. *Journal of Physiology-Paris*, 103(3):195–210, 2009.

[17] Robert J. Telban and Frank M. Cardullo. Motion cueing algorithm development: Human-centered linear and nonlinear approaches. Technical report, State University of New York, 2005.

[18] The MathWorks, Inc. *Simscape™ Multibody™ User's Guide*, r2018b edition, 2018.

[19] Lorenzo Vannucci, Egidio Falotico, Silvia Tolu, Paolo Dario, Henrik Hautop Lund, and Cecilia Laschi. *Living Machines 2016: Biomimetic and Biohybrid Systems*, chapter Eye-Head Stabilization Mechanism for a Humanoid Robot Tested on Human Inertial Data, pages 341–352. Springer, 2016.

[20] Vishesh Vikas and Carl Crane. Bioinspired dynamic inclination measurement using inertial sensors. *Bioinspiration & Biomimetics*, 10:036003, 2015.

[21] M. Zebenay, V. Lippi, and T. Mergener. Human-like humanoid robot posture control. In *12th International Conference on Informatics in Control, Automation and Robotics (ICINCO 2015)*, pages 304–309, 2015.